Reaction Kinetics and Mechanism of Catalyzed Hydrolysis of Waste PET Using Solid Acid Catalyst in Supercritical CO_2

Xue-Kun Li, Hui Lu, Wen-Ze Guo, Gui-Ping Cao, Hong-Lai Liu, and Yun-Hai Shi
UNILAB, State Key Laboratory of Chemical Engineering, East China University of Science and Technology, Shanghai 200237, People's Republic of China

DOI 10.1002/aic.14632
Published online October 1, 2014 in Wiley Online Library (wileyonlinelibrary.com)

Hydrolysis of waste poly(ethylene terphthalate) (PET) using solid acid catalyst in $SCCO_2$ is presented in this work for the first time. The mechanism of PET chains scission was proved to be a combination of chain end and random chain scission by Fourier transform - infrared spectroscopy (FT-IR) and titration analysis. A new reaction kinetics model of PET hydrolysis in $SCCO_2$ was setup by introducing the Arrhenius equation into an ordinary reaction rate equation, the frequency factor and apparent activation energy were expressed in terms of temperature and CO_2 pressure, respectively. With this reaction kinetics model, the effects of temperature, and pressure were investigated. An interesting mechanism was proposed to describe the reaction process that both water molecules and hydroniums were carried and penetrated into the amorphous regions of the swollen PET by $SCCO_2$, subsequently hydrolysis reaction preferentially took place in the amorphous regions of both surface and bulk of PET matrix. © 2014 American Institute of Chemical Engineers *AIChE J*, 61: 200–214, 2015

Keywords: PET hydrolysis, supercritical carbon dioxide, solid acid catalyst, CO_2-induced crystallization, amorphous and crystalline regions

Introduction

As one of the most-produced polymers, poly(ethylene terphthalate) (PET), is a thermoplastic polymer resin of the polyester family and is widely used in synthetic fibers as well as beverage, food, and other liquid containers. To minimize the plastic pollution, the world plastics industry has always been concerning the recycling of waste PET.[1] Unlike the physical recycling, the chemical recycling makes PET degraded into monomer units (i.e., depolymerization) or randomly ruptured into larger chain fragments (i.e., random chain scission),[2] and the fundamental principle of depolymerization is to cleave the functional ester groups of PET. The most common techniques for depolymerization of polyester contain hydrolysis, glycolysis, methanolysis, and aminolysis,[2–5] where the hydrolysis can be further divided into three categories, such as acid, alkaline, and neutral hydrolysis. In this work, we will focus on the acid hydrolysis.

Acid hydrolysis is performed most frequently using concentrated acid, for instance, nitric acid, phosphoric acid, and sulfuric acid. Various kinds of depolymerization kinetics have been developed and validated in many studies. Campanelli et al.[6] suggested that it was possible for melted PET to be depolymerized completely to monomer at the temperature above 265°C for the initial mass ratio of H_2O to PET above 5:1, and this ratio would affect the equilibrium parameter of the kinetics model. Lin et al.[7] investigated the kinetics for depolymerization of poly(methylmethacrylate) (PMMA) in concentrated HNO_3 (69–70%) by microwave irradiation technique, they found that temperature could affect the type of kinetics, that is, the zero-order reaction was observed dominantly at 150–170°C, while the first-order reaction dominated at 180 and 200°C. Yoshioka et al.[8] proposed an acid hydrolysis of waste PET powder in H_2SO_4 at the temperature ranged from 150–190°C for different reaction time (1–12 h), and their results revealed that the degree of PET degradation increased with the increment of H_2SO_4 concentration and the reaction temperature. They introduced a shrinking-core model to investigate the hydrolytic mechanism and kinetics, and this model was also adopted to the hydrolysis of PET using HNO_3.[9] Mishra et al.[10] used H_2SO_4/H_3PO_4 compound to make the degree of PET hydrolysis achieve 97.8% at 140°C and atmosphere pressure for 140 min, and they found that the apparent rate constant of hydrolysis reaction would begin to reduce when the initial particle diameter of PET was >150 μm. Unfortunately, although increasing the concentration of mineral acid could enhance the efficiency of hydrolysis, the process for recycling large amounts of concentrated acid and the purification of ethylene glycol (EG) from the liquid acid would become very costly, furthermore, the concentrated acid also accelerated the process of the corrosion of equipment.[2,4] It is significant to develop an environmental friendly strategy for chemical recycling of PET, for instance, using other catalyst to replace concentrated acid. In recent years, ionic liquids had been used as the functional phase transfer catalyst to hydrolyze PET, with the outstanding catalytic activity, the conversion was almost reach to 100%.[11,12] However, the ingredients of ionic liquids were relatively complex and costly, and might have a long way to be industrialized.

Additional Supporting Information may be found in the online version of this article.

Correspondence concerning this article should be addressed to G.-P. Cao at gpcao@ecust.edu.cn.

Compared to liquid acid and ionic liquid, solid acid catalyst has obvious advantages, including convenient preparation, easy regeneration, environmentally safe disposal, and improving the equipment corrosion problems caused by liquid concentrated mineral acid.[13,14] Due to these advantages, solid acid catalyst has been widely used in many chemical reactions, of course, including degradation of polymers.[15] Song et al.[16] used different metal oxides as solid catalysts to hydrolyze grain PET, and the conversion could reach to 90.9% with tin oxides at 200°C for 210 min. However, in the procedures of separation and purification of the products, excessive wastewater would increase energy consumption, in addition, all the catalyst seemed not to be recycled for reuse. As described earlier, increasing the concentration of acid can enhance the efficiency of PET hydrolysis, to enhance the acid strength of solid acid catalysts, metal oxides, such as ZrO_2, TiO_2, SnO_2, and Fe_2O_3, were pretreated by sulfuric acid, then exhibited stronger surface acidity and catalytic activity, which were called solid super-acid catalyst.[13,14,17–21] To our knowledge, using the solid metal oxide super-acid catalyst to catalyze the hydrolysis of PET has not been previously reported. Therefore, we prepared sulfated TiO_2 (SO_4^{2-}/TiO_2) as catalyst to investigate the hydrolysis of waste PET in this work.

As we know, there is no surface tension, that is, liquid/gas phase boundary, in a supercritical fluid, due to this unique properties of supercritical fluid, it can diffuse into solids like a gas, and dissolve materials like a liquid. A large amount of researches had demonstrated the superiority of supercritical fluid in the depolymerization of waste PET, such as the hydrolysis with supercritical water[22–24] and methanolysis with supercritical methanol.[24–28] All those results exhibited that PET could be almost completely depolymerized within 150 min, however, it is not energy-efficient to satisfy the supercritical state of supercritical water ($T_c = 374.3$°C, $P_c = 22.0$ MPa) and supercritical methanol ($T_c = 239.5$°C, $P_c = 8.1$ MPa), which limits the application of them. Carbon dioxide has many interesting properties such as the easily accessible critical point ($T_c = 31.4$°C, $P_c = 7.38$ MPa), nonflammable, nontoxic, low cost, chemical inertness, easy availability, environmentally benign nature, and the relatively significant ability of sorption and diffusion into semicrystalline polymers, which has made CO_2 used as a popular physical modification agent in the applications of polymer modification,[29–36] of course, including PET.[36–42] Like other CO_2-polymer systems, due to the plasticizing effect of CO_2, dissolving CO_2 in PET will modify the properties in both glassy and rubbery states of PET, such as swelling the PET matrix to expand the free volume for the mobility of chain segments,[37,40] controlling the structure of PET microcellular foams,[30,38,41] depressing the glass transition temperature and the crystallization temperature,[39,42] inducing crystallization of amorphous PET,[38,43] and changing the crystallization kinetics,[39,43] besides, the waste PET could be used to produce activated carbon with CO_2 as activating agent.[44] Considering these significant interactions between CO_2 and PET, we believe that CO_2 must affect the reaction kinetics and mechanism of the PET hydrolysis when supercritical CO_2 ($SCCO_2$) is introduced into the reaction system.

In this work, an interesting mechanism for the hydrolysis of waste PET using solid super-acid catalyst (SO_4^{2-}/TiO_2) in $SCCO_2$ was introduced. As a driven agent of the entire reaction, $SCCO_2$ was supplied to a sealed high-pressure vessel in which a cell holder separately loaded with water and the mixture of PET and catalyst was placed. There would be three dominate effects that $SCCO_2$ can make, (1) $SCCO_2$ is capable of swelling the PET matrix to provide sufficient space for the bulk reaction, (2) $SCCO_2$ transports the water to the surface of PET/catalyst mixture and adsorbs on it, then the hydroniums generated from the Bronsted-acid site of solid acid catalyst, (3) both water molecules and hydroniums carried by $SCCO_2$ penetrates into the amorphous regions of PET matrix and finally results in the hydrolysis reaction occurred both on the surface and in the bulk of PET. The degree of hydrolysis, that is, the conversion of PET, was determined by the weight method, while the conversion and selectivity of hydrolysis products were characterized and evaluated by gas chromatograph - mass spectrometry (GC-MS), liquid chromatography - mass spectrometry (LC-MS), and Fourier transform - infrared spectroscopy (FT-IR) analysis, respectively. A new reaction kinetics model is subsequently proposed by introducing the Arrhenius equation into an ordinary reaction rate equation, and then expressing the frequency factor and apparent activation energy in the Arrhenius equation in terms of temperature and CO_2 pressure, respectively. After the related parameters are obtained by least-squares estimation of the experimental data, this reaction kinetics model can be used to correlate and predict the temperature and CO_2 pressure distribution in the catalyzed hydrolysis of waste PET. The FT-IR and end-group titration analysis were used to detect the scission behavior of PET chains during hydrolysis reaction. To verify the interesting mechanism introduced in this work, the morphologies of surface and cross section of the PET flakes for the different degree of hydrolysis are observed by the scanning electron microscopy (SEM) technique, and the results agree well with the assumption.

Reaction Kinetics Model of PET Hydrolysis in $SCCO_2$

Waste PET flake was hydrolyzed in water to yield the terephthalic acid (TPA) and EG, according to the following chemical reaction (Figure 1). Since water used in the entire process of reaction is excess, the reaction rate can be expressed by the ratio of residual mass ($m_{t,\mathrm{PET}}$) to initial mass ($m_{0,\mathrm{PET}}$) of PET changed vs. time, which can be written as

$$r = -\frac{d(m_{t,\mathrm{PET}}/m_{0,\mathrm{PET}})}{dt} = kf(m_{t,\mathrm{PET}}/m_{0,\mathrm{PET}}) \tag{1}$$

where $f(m_{t,\mathrm{PET}}/m_{0,\mathrm{PET}})$ depends on the particular decomposition mechanism, k is the apparent reaction rate constant. The degree of PET hydrolysis (D_h) can be defined as

$$D_h = \frac{m_{0,\mathrm{PET}} - m_{t,\mathrm{PET}}}{m_{0,\mathrm{PET}}} \tag{2}$$

then

$$\frac{m_{t,\mathrm{PET}}}{m_{0,\mathrm{PET}}} = 1 - D_h \tag{3}$$

here we assume $f(m_{t,\mathrm{PET}}/m_{0,\mathrm{PET}}) = (m_{t,\mathrm{PET}}/m_{0,\mathrm{PET}})^n$, n represents the order of the reaction, then $f(1-D_h) = (1-D_h)^n$, Eq. 1 can be written as

$$-\frac{d(1-D_h)}{dt} = k(1-D_h)^n \tag{4}$$

when $n = 1$, by integrating Eq. 4, we can obtain

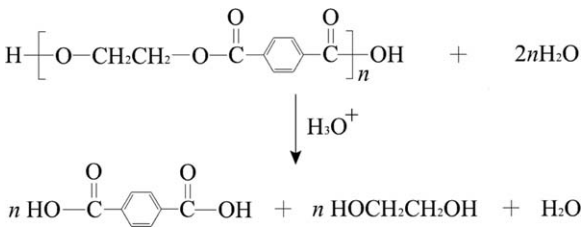

Figure 1. Hydrolysis of PET.

$$\ln(1-D_h)=-kt \tag{5}$$

then

$$D_h=1-\exp(-kt) \tag{6}$$

when $n\neq 1$, by integrating Eq. 4, we should obtain

$$\frac{(1-D_h)^{1-n}}{1-n}=-kt \tag{7}$$

then

$$D_h=1-[(n-1)kt]^{\frac{1}{1-n}} \tag{8}$$

To describe the effect of temperature, according to the Arrhenius equation, k can be shown as

$$k=k_0\exp\left(-\frac{E}{RT}\right) \tag{9}$$

where k_0 is the frequency factor, which describes the probability of effective regular arrangement among PET segments during their movements. Due to the hydrolysis of PET starts with the scission of polymer chains, E is the apparent activation energy for the movement of polymer chains. R is the gas constant, and T is the temperature in unit of Kelvin.

PET is a kind of semicrystalline thermoplastic polyester, which is composed of amorphous and crystalline regions. With the assistance of $SCCO_2$, the sorption of water is only possible in the amorphous region, simultaneously, the plasticizing effect of $SCCO_2$ can reduce the glass transition temperature of PET to induce the chain segments in amorphous region to become regular, that is, the so-called CO_2-induced PET crystallization. Therefore, the increment of crystallinity of PET cannot be ignored in the kinetic study of hydrolysis.[45] According to the early studies,[46,47] the apparent activation energy for the homogeneous nucleation is related to the difference of Gibbs free energy between the amorphous and crystalline phases, and the apparent activation energy can be expressed by the following form[48]

$$E(P)=\frac{16\pi}{3}\frac{\sigma^3}{\Delta G^2}=\frac{1}{a+bP+cP^2} \tag{10}$$

where a, b, and c are the model parameters, and the value of activation energy of crystallization is equal to the apparent activation energy for the movement of polymer chains.

Because the temperature can directly affect the movement ability and effective regular arrangement of PET segments, which will then affect the value of k_0, here we assume the k_0 can be related to temperature in the following equation

$$k_0(T)=\alpha+\beta T+\gamma T^2 \tag{11}$$

where α, β, and γ are the model parameters. Thus, Eq. 9 can be modified by Eq. 12

$$k(T,P)=k_0(T)\exp\left(-\frac{E(P)}{RT}\right) \tag{12}$$

then Eqs. 6 and 8 can be, respectively, modified in the form of

$$D_h=1-\exp[-k(T,P)t] \quad \text{for} \quad n=1 \tag{13}$$

and

$$D_h=1-[(n-1)k(T,P)t]^{\frac{1}{1-n}} \quad \text{for} \quad n\neq 1 \tag{14}$$

In summary, the reaction kinetics model of PET hydrolysis in $SCCO_2$ can be described by two groups of equations, that is, Eqs. 10–13 or Eqs. 10–12 and 14.

Experimental

Materials

Nitrogen (UHP grade, 99.99%) and CO_2 (purity > 99.9%) were purchased from Hukang Gas Co. Ethanol (AR grade, 99.7%), dimethyl sulfoxide (DMSO; AR grade, 99.0%), $NH_3\cdot H_2O$ (AR grade, 25.0–28.0%), 1,1,2,2-tetrachloroethane (AR grade, 99%), acetic anhydride (AR grade, 98.5%), phenol (AR grade, 99%), pyridine (AR grade, 99%), benzene (AR grade, 99.5%) were obtained from Shanghai Lingfeng Chemical Reagent Co., $Ti(SO_4)_2$ (CP grade, 96.0%), KOH (AR grade, 85%) were purchased from Sinopharm Chemical Reagent Co. Homemade deionized water was obtained by doubly distilling water pretreated by reverse osmosis.

Waste PET soft-drink bottles (transparent, $\bar{M}n\approx 23,100$ g/mol), without polypropylene labels, were obtained from the Coca-Cola company. Each bottle was shredded into flakes ($4\times 4\times 0.4$ mm^3), and cleaned in detergent, ethanol, and deionized water with an ultrasonic vibration cleaner for 3 min, respectively, then vacuum-dried at 80°C for 12 h. After this cleaning process, the clean PET flakes were sealed in a zip-lock bag, for all the hydrolysis experiments.

Apparatus and operation

The catalyzed hydrolysis of PET using solid acid catalyst in $SCCO_2$ was carried out in a custom-made batch high-pressure vessel, which was a thick-walled stainless steel cylinder with an internal volume of 300 mL and a maximum working pressure of 30 MPa. To make the PET/catalyst mixture was separated from water, which would prevent water obstructing the diffusion of $SCCO_2$ into PET matrix, a custom-made cell holder with two separate glass cells was placed vertically in the vessel. The pressure vessel was entirely immersed in a temperature-controlled oil bath to maintain a temperature accuracy of ±0.1°C. A thermocouple was placed in the vessel to measure the temperature of fluid, and the pressure was measured by a pressure transducer (LEEG, SMP131, 0.2% F.S accuracy). A custom-made buffer tank with a heater was connected after the CO_2 cylinder to supply high-pressure CO_2 to the vessel.

Preparation of the SO_4^{2-}/TiO_2 solid super-acid catalyst

The sulfated metal oxides (SO_4^{2-}/M_xO_y) are usually prepared by first precipitating the hydroxides from corresponding aqueous metal salt solution, after washing, filtering, and drying, the hydroxides are treated with a solution of H_2SO_4 or $(NH_4)_2SO_4$, finally the sulfated metal oxides are obtained by calcining the dried sulfated hydroxides at the temperature

of 500–650°C.[13] In this work, $Ti(SO_4)_2$ was used as the starting material to prepare the SO_4^{2-}/TiO_2, which could eliminate the step of H_2SO_4 treatment.

The typical procedure for preparing the SO_4^{2-}/TiO_2 catalyst is as follows. (1) Dissolving the titanium sulfate ($Ti(SO_4)_2$) in deionized water at the temperature of 30°C as the mass ratio of $Ti(SO_4)_2$ (1):H_2O (10), to obtain the $TiOSO_4$ aqueous solution. (2) Dropping diluted $NH_3 \cdot H_2O$ (10%) to the $TiOSO_4$ aqueous solution to precipitate $Ti(OH)_4$ and generate $(NH_4)_2SO_4$ solution until the pH value reached to 8 with vigorous agitating. (3) After aging for 24 h, the precipitated $Ti(OH)_4$ was filtered out from the $(NH_4)_2SO_4$ solution, simultaneously, a mount of NH_4^+ cations and SO_4^{2-} anions adsorbed on the surface of precipitated $Ti(OH)_4$, which could be expressed by $NH_4^+|SO_4^{2-} \cdot Ti(OH)_4$. (4) After dried at 110°C for 12 h, $Ti(OH)_4$ changed to the amorphous $TiO_2 \cdot xH_2O$, which was the precursor of TiO_2, then grinding the dried $NH_4^+|SO_4^{2-} \cdot TiO_2 \cdot xH_2O$ into powder (particle size < 100 μm). (5) By calcining the dried $NH_4^+|SO_4^{2-} \cdot TiO_2 \cdot xH_2O$ powder at the temperature of 500°C for 6 h, NH_4^+ cations were decomposed and SO_4^{2-} anions chelated to TiO_2, then the anatase solid super-acid catalyst, SO_4^{2-}/TiO_2, was obtained.[13] The acidity of solid acid catalyst was 0.43×10^{-3} mol/g, which was determined by temperature - programmed desorption (TPD) (Micromeritics, Autochem II 2920), and the surface area and pore volume were 46.76 m^2/g and 0.17 cm^3/g, which were determined by Brunner Emmet Teller (BET) (ASAP 2020M+C), respectively.

Determination of the degree of PET hydrolysis

Before each run, the initial mass of PET flakes ($m_{0,PET}$) and solid acid catalyst (m_{cat}) were, respectively, measured using an analytical balance (Mettler Toledo, AB 104-N) and mixed. The mixture and deionized water were placed into the pressure vessel by loading them, respectively, in different cells of the cell holder as the following mass ratio, PET (1):catalyst (0.1):H_2O (10). At the end of the hydrolysis for various reaction conditions, that is, temperature, pressure, and time of reaction, the pressure vessel was transferred from the oil bath to a cold-water bath (5–10°C) to be cooled for 30 min, then the pressure was released to atmosphere at a low speed (0.1 MPa/min). This step aimed at preventing EG/H_2O compound carried by $SCCO_2$ releasing out from vessel as much as possible. Then, taking the two cells out from the vessel, and the product in the mixture cell was washed thrice with cold deionized water (5–10°C) to remove the water-soluble components (mainly EG monomer), the solid product was filtered out, then dried in vacuum at 80°C for 6 h. The dried solid product was then washed thrice with DMSO solvent to remove TPA, the residual PET and catalyst were filtered and dried in vacuum at 120°C for 6 h to obtain the mass of residual PET and catalyst ($m_{t,PET/cat}$), the mass of residual PET could be calculated via $m_{t,PET} = m_{t,PET/cat} - m_{cat}$, while the mixture of residual PET and catalyst can be directly reused for the next experiment, and the degree of PET hydrolysis, D_h, could be obtained by Eq. 2.

It was worth detecting whether EG existed in all the liquid phase, including water cell, mixture cell, and the inner wall of vessel. Fortunately, after analyzing, it was found that EG only existed in the mixture cell. A substantial volume of diluted EG could be recovered by distillating the EG/H_2O solution,[49–52] the distillated EG was determined by weight method, and the molar yield of EG could be calculated by[8]

$$\text{molar yield of EG } (\%) = \frac{n_{t,EG}}{n_{0,EG}} \times 100 \quad (15)$$

where $n_{t,EG}$ and $n_{0,EG}$ referred to the measured and theoretical number of EG moles, produced by complete hydrolysis of PET, respectively.

TPA could be precipitated by dropping deionized water to the TPA/DMSO solution, of course, the distilled water obtained from the EG/H_2O solution was still used in this step, after filtering, the TPA could be obtained by dried in vacuum at 120°C to a constant weight, the recovered TPA was determined by weight method, and the molar yield of TPA could be calculated by[8,53]

$$\text{molar yield of TPA } (\%) = \frac{n_{t,TPA}}{n_{0,TPA}} \times 100 \quad (16)$$

where $n_{t,TPA}$ and $n_{0,TPA}$ referred to the measured and theoretical number of TPA moles, produced by complete hydrolysis of PET, respectively. The DMSO solvent also could be recovered by distillating the DMSO/H_2O solution. The hydrolysis products were qualitatively analyzed by GC-MS (Agilent, GC6890/MSD5975) and LC-MS (Agilent 6120), respectively. The difference of groups between raw and residual PET as well as the purity of EG and TPA all could be characterized by FT-IR (Nicolet 6700).

Surface and cross-sectional morphology analysis of PET flakes

To observe the surface and cross-sectional morphology of PET flake, four samples with different degree of hydrolysis were prepared under different treatment conditions. The first one was a clean original PET flake, the other three underwent hydrolysis at 160°C and 15 MPa for 2, 3, and 9 h, respectively, in the high-pressure vessel. After this operation, the pressure was released to atmosphere at a low speed (0.1 MPa/min), which could prevent the flake morphology from changing by the foaming effect so as to ensure the morphological changes only caused by hydrolysis. Then, each flake was cleaned in ethanol and water with ultrasonic vibration for 1 min, respectively, to remove EG and catalyst adhered on the surface of TPA and residual PET. For the observation of cross-sectional morphology, an entire flake was broken into two or more pieces after it had been cooled in liquid nitrogen for 15 s to keep the integrity of the cross-sectional morphology from being destroyed during breaking. After dried at 80°C for 6 h, the surface and cross-sectional morphology of each sample was characterized by SEM (FEI, Nova NanoSEM 450).

Other experiment and analysis

To verify the sorption of CO_2 into PET and the swelling of PET flake, a series of swelling experiments were carried out in an high-pressure view cell with a charge coupled device (CCD) camera, the apparatus and corresponding operation could be find in our previous work.[54]

The end-group titration method was used to determine the number average molecular weight of fresh and residual PET, the operational details were provided in the Supporting Information.

Results and Discussion

Reliability of hydrolysis results

In any chemical degradation of PET, it always starts with the scission of polymer chains, which is subsequently

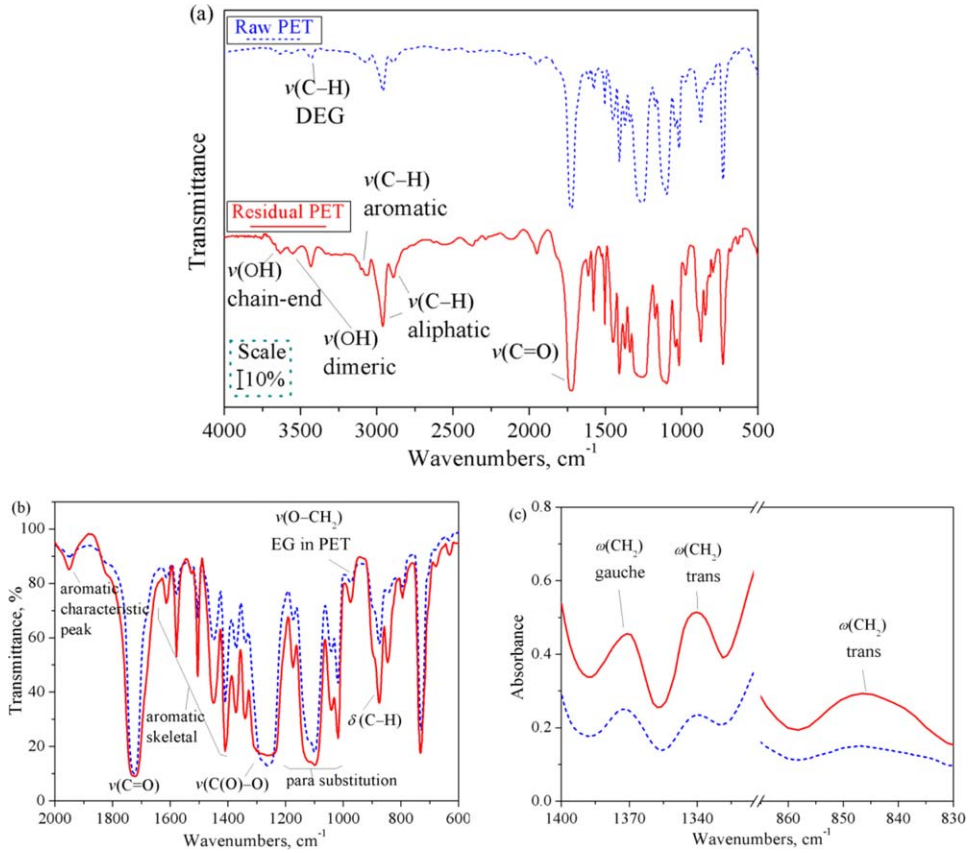

Figure 2. FT-IR spectra of the original and residual PET in the region of (a) 500–4000 cm^{-1}, (b) 600–2000 cm^{-1}, and (c) 830–1400 cm^{-1}, where the residual PET was hydrolyzed at 160°C and 15 MPa for 2 h, $D_h = 39.21\%$, then cleaned by H_2O and DMSO, respectively, and dried to remove EG and TPA.

[Color figure can be viewed in the online issue, which is available at wileyonlinelibrary.com.]

depolymerized to the oligomers, and ultimately depolymerized to different monomers, such as bis (2-hydroxyethyl) terephthalate,[55] dimethyl terephthalate,[25] TPA, and EG. Mancini and Zanin[56] concluded that PET hydrolysis occurred preferentially at the chain ends and surface of PET, the controller mechanism depended on the diffusion of acid into the polymer structure. Ballara and Verdu[57] also proposed that the rate of a specific chain-end process was higher than the random one, and the rate of hydrolysis was higher at terminal than at internal ester groups. However, Launay et al.[58] used a classical second-order kinetics to expressed that the random chain scission process seemed to be sufficient to describe the PET hydrolysis behavior.

FT-IR technique can be used to determine the scission mode of chains of PET hydrolyzed in $SCCO_2$, and a typical FT-IR spectrum of original and residual PET is shown in Figure 2. As the transmittance intensity of the peak at 1270 cm^{-1} band, which represented the stretching vibration of ester group, ν(C(O)—O), decreased evidently due to the scission of ester groups after PET incomplete hydrolysis, it would be taken for the reference peak to analyze the change of other peaks in FT-IR spectra after PET incomplete hydrolysis. It was found that most of peaks at different bands had evidently become broadened or strengthened, including 730 cm^{-1} band (the out of plane deformation of the two carbonyl substituents on the benzene ring), 850, 875, and 878 cm^{-1} bands (C—H deformation of two adjacent coupled hydrogens on benzene ring, δ(C—H)), 1017, 1040, 1100, and 1175 cm^{-1} bands (the skeletal vibration of benzene ring with para substitution), 1410, 1450, 1505, 1578, and 1615 cm^{-1} bands (the aromatic skeletal vibration), 1724 cm^{-1} band (the stretching vibration of all carbonyl groups in PET, ν(C═O)), 1950 cm^{-1} band (the aromatic characteristic peak), 2880 and 2960 cm^{-1} bands (aliphatic C—H stretching vibration, ν(C—H)), and 3060 cm^{-1} band (aromatic C—H stretching vibration, ν(C—H)). Due to the scission of polymer long chains, the negative effect between groups was weakened, therefore, the stretching, bending, wagging, or other type of vibration of some groups was enhanced, and the corresponding peaks expressed stronger transmittance intensity. Especially, the transmittance intensity of several characteristic peaks, such as 975 cm^{-1} band (O—CH_2 stretching vibration of EG segment in PET, ν(O—CH_2)), 3440 cm^{-1} band (O—H stretching vibration of diethylene glycol [DEG] end group), 3550 cm^{-1} band (the stretching vibration of hydrogen bond between OH in carboxyl groups of dimeric) and 3630 cm^{-1} band (the stretching vibration of OH groups in the chains-end), were also enhanced after PET incomplete hydrolysis, which indicated that the random scission of PET long chains resulted in more end groups of PET were exposed. Conversely, along with the random scission of PET long chains, the monomers (TPA and EG) were also obtained due to the scission of ester groups in the chains end. All the above different bands assignment for the infrared spectrum of PET had been described in other researchers' works.[59–61]

As hydroniums carried by $SCCO_2$ diffuses into the amorphous regions of PET matrix and induces both the terminal

Table 1. Degree of PET Hydrolysis and Corresponding Molar Yields of TPA, EG, and DEG at 160°C and 15 MPa for Different Reaction Time

t, h	D_h of PET (%)	Molar Yield of TPA (%)	Molar Yield of EG (%)	Molar Yield of DEG (%)
2	39.21	38.33	38.18	–
3	72.54	72.37	71.56	–
3	74.35	73.85	73.61	–
3	73.26	72.98	72.87	–
6	94.35	94.19	87.59	5.85
6	94.09	93.90	87.02	5.92
6	93.01	92.92	86.23	5.24
9	96.89	96.05	88.29	7.02
12	99.86	99.19	90.78	7.84

and internal ester groups to cleave, therefore, the process of PET hydrolysis in $SCCO_2$ is a combination of chain end and random chain scission, which could also be described by the end-group titration method (details are provided in the Supporting Information), the similar result had been suggested in liquid-phase polymer degradation by McCoy and Madras.[62]

Another meaningful phenomenon should be noticed, the peaks at 846 and 1340 cm^{-1} bands (Figure 2c) are assigned to the CH_2 wagging mode in the trans conformers, while gauche conformers appears at 1370 cm^{-1} band, the crystallinity of PET can be estimated by calculating the ratio of gauche to trans conformers, that is, A_{1370}/A_{846} or A_{1370}/A_{1340}, where "A" is the integral absorbance of the different peak band.[38,63] For the original sample, $A_{1370}/A_{846} = 1.90$ and $A_{1370}/A_{1340} = 1.22$, while for the residual sample, $A_{1370}/A_{846} = 1.76$ and $A_{1370}/A_{1340} = 0.96$. It was found that both A_{1370}/A_{846} and A_{1370}/A_{1340} values decreased after PET was incompletely hydrolyzed in $SCCO_2$, which indicated the crystallinity of PET increased,[38,63] that is, so-called CO_2-induced crystallization of PET.

To qualitatively and quantitatively detect the hydrolysis products, LC-MS and GC-MS analysis were used to characterize the products (details are provided in the Supporting Information). The degree of PET hydrolysis and corresponding molar yields of TPA, EG, and DEG at 160°C and 15 MPa for different reaction time are exhibited in Table 1. At the time range below 6 h, the molar yields of both TPA and EG were slightly lower than the degree of PET hydrolysis, which could be attributed to the slight mass loss of TPA and EG in the procedures of separation and purification, while this result indicated that the hydrolysis of PET proceeded quantitatively according to the reaction route expressed in Figure 1. As the hydrolysis continued, however, the difference between the molar yields of TPA and EG increased with increasing time at the reaction time range above 6 h. Two reasons were referred to explain this result, one was due to the secondary reaction catalyzed by TPA, EG was transformed to DEG,[25] another was carbonization of EG by concentrated sulfuric acid.[8] However, in this work, the reason of EG was dehydrated to DEG could be attributed to the catalyst acidity rather than the above two reasons (details are provided in the Supporting Information).

Figure 3a illustrates the typical FT-IR spectra of the TPA recovered in this work. The transmittance peaks in the region of 2500–3000 cm^{-1} (2549, 2665, 2816, 2822, and 2981 cm^{-1} bands) denoted the stretching vibration of OH, ν(OH), in carboxyl groups, especially the transmittance peaks at 3066 and 3101 cm^{-1} bands represented the ν(OH) in carboxyl groups of dimeric TPA. Due to the conjugated effect of the carboxyl groups and benzene rings, the ν(C═O) in of carboxyl groups evidently appeared at 1684 cm^{-1} bands. The skeleton vibration of benzene ring could be found at 1509 and 1574 cm^{-1}, while the peaks at 730 and 779 cm^{-1} bands were attributed to the out-of-plane blending vibration of C—H, γ(C—H), in benzene ring after the para-hydrogen were substituted. All these characteristic and other detailed transmittance peaks of TPA were almost the same with the results of Téllez et al., which reported the detailed FT-IR spectra of the solid pure TPA,[64] therefore, the TPA recovered in this work had a high purity.

Figure 3b illustrates the typical FT-IR spectra of the EG recovered in this work. The skeleton vibration of EG was observed at 864 cm^{-1}, 1085 and 1042 cm^{-1} bands, which denoted the stretching vibration of C—O, ν(C—O), while the peaks at 1334, 1402, 1459, 2880, and 2946 cm^{-1} bands represented the $\nu(CH_2)$, and the wide peak around 3386 cm^{-1} band was the ν(OH). It was worth noting that the peak at 1647 cm^{-1} band was the characteristic transmittance peak of DEG, which proved that a certain amount of DEG indeed existed in EG recovered in this work. Conversely, due to the hygroscopicity of EG, the presence of a micro amount of H_2O in EG could also be understood.

In summary, using solid acid catalyst and $SCCO_2$, waste PET bottles can be almost completely hydrolyzed to monomers of TPA and EG, although a little amount of EG will be transformed to DEG, while DMSO can be recovered by distillating the DMSO/H_2O solution for reuse. Therefore, the entire process of PET hydrolysis and products extraction is

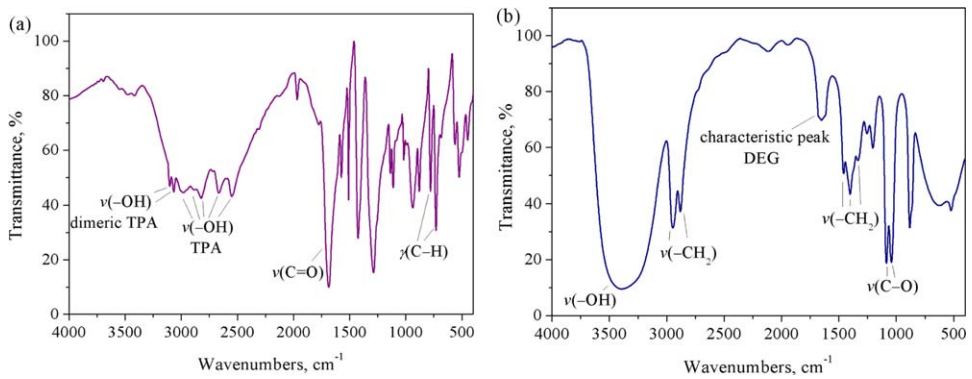

Figure 3. FT-IR spectra of (a) TPA and (b) EG recovered by PET hydrolysis at 160°C and 15 MPa for 12 h.

[Color figure can be viewed in the online issue, which is available at wileyonlinelibrary.com.]

Table 2. Estimated Parameters for Reaction Kinetics Model

No.	Parameter	Value
1	n	1.00
2	α	11.64
3	β	−0.19
4	γ	4.63×10^{-4}
5	a	7.05×10^{-5}
6	b	-2.58×10^{-6}
7	c	2.31×10^{-7}

an environmentally benign process. Besides duplicate experiments for the determination of degree of PET hydrolysis at the reaction time of 3 and 6 h, respectively (Table 1), also verified the reproducibility of the method used in this work.

Reaction kinetics of PET hydrolysis in $SCCO_2$

To obtain the intrinsic kinetics model of PET hydrolysis in $SCCO_2$, seven parameters, that is, n, α, β, γ, a, b, and c, should be estimated by fitting the experimental data. The data used for fitting in this work were over the ranges of 8–15 MPa, 100–160°C, and 3–12 h. A nonlinear least-squares method, which based on the Levenberg–Marquardt algorithm, was used to estimate these parameters. The results are shown in Table 2.

The apparent activation energy and frequency factor for PET hydrolysis in $SCCO_2$ can be calculated by Eqs. 10 and 11, respectively, and the results are shown in Figure 4. The frequency factor increased with increasing temperature. As described earlier, the values of frequency factor indicated the probability of effective regular arrangement among polymer chains during their movement, while the melting temperature of PET (250–255°C) was much higher than the experimental temperature in this work, that is, PET was hydrolyzed in rubbery state. Therefore, as temperature increased, the movement ability of polymer chains was enhanced, which accelerated the scission of chains in hydrolysis. The apparent activation energy decreased with increasing pressure, as the Gibbs free energy of polymer chains were increased by introducing CO_2 into the amorphous regions of polymer. As the apparent activation energy decreased, the movement ability of polymer chains was also enhanced. Therefore, both the increasing frequency factor and the decreasing apparent activation energy can improve the hydrolysis rate. For the parameter $n = 1$, which indicates that the hydrolysis of PET using solid acid catalyst in $SCCO_2$ was much more similar to a first-order reaction.[4,6,25,65–67]

The experimental and model values of degree of PET hydrolysis at different temperatures and pressures for different times are shown in Figure 5. In the time range of 3–12 h, the experimental values are evenly distributed on both sides of the model curves, that is, deviations between experiment and model appear to be random. At the temperature of 100°C, it can be predicted that it would be hard to make PET hydrolyzed completely, even for higher pressure and a

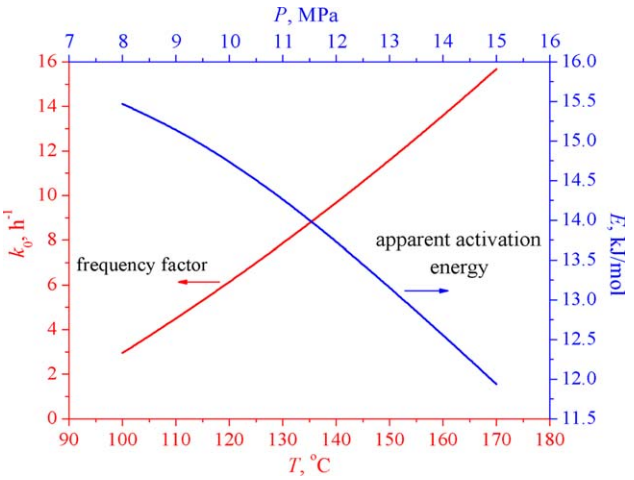

Figure 4. Model values of frequency factor (k_0) vs. temperature and apparent activation energy (E) vs. pressure for the hydrolysis of PET in $SCCO_2$.

[Color figure can be viewed in the online issue, which is available at wileyonlinelibrary.com.]

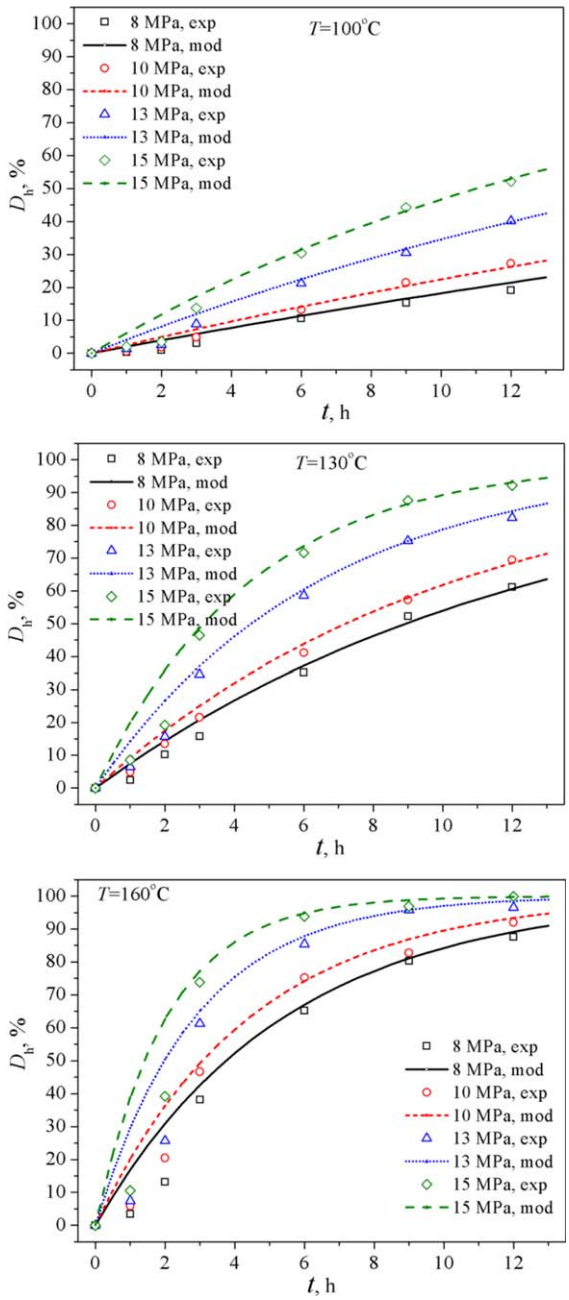

Figure 5. Degree of PET hydrolysis vs. time at different temperatures and pressures.

[Color figure can be viewed in the online issue, which is available at wileyonlinelibrary.com.]

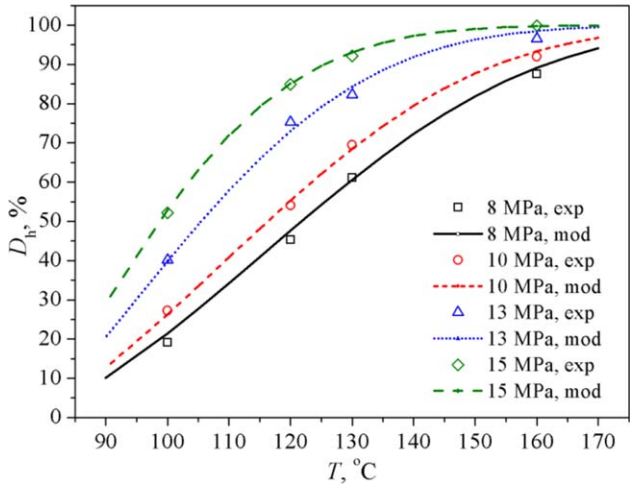

Figure 6. Degree of PET hydrolysis after 12 h vs. temperature at different pressures.

[Color figure can be viewed in the online issue, which is available at wileyonlinelibrary.com.]

long enough time. Temperature could affect the polymer chain flexibility and diffusion of small molecules, therefore, an effective operation for increasing the free volume of PET and enhancing the diffusion of H_2O into PET is to increase temperature. Furthermore, at a given temperature and pressure, it was found that the change of experimental D_h values vs. time was a S-shape curve. In the initial stage of the reaction, PET was swollen by CO_2, simultaneously, most of polymer chains began to cleave after H_2O carried by $SCCO_2$ and penetrated into the amorphous regions of PET, therefore, D_h increased slightly. Viana et al.[68] considered that the lower conversion at initial reaction time could be attributed to the apparent reaction equilibrium between oligomers and unreacted PET at lower temperature, besides the diffusion process should be taken into account. Then, most of the ester groups of short chains in the amorphous regions started to be rapidly hydrolyzed to monomers, that is why D_h increased sharply in the second stage of reaction. At the last stage, hydrolysis occurred mainly at the crystalline regions, however, moisture could not diffused into the crystalline regions, which slowed the rate of hydrolysis.[45]

In the time range of 0–3 h, the experimental values significantly deviated from the model curves, in fact, we believed that the sorption of CO_2 into PET and the swelling of PET were more significant than the hydrolysis of PET in this time range, therefore, these data would not be used for fitting. After measuring the volume change of PET flake at different time, the results of the swelling ratio of PET in $SCCO_2$ at 15 MPa for different temperature and time were shown in Figure S6 of Supporting Information. A similar result could be found in Schnitzler's research,[40] the corresponding equilibrium time for the swelling of PET decreased with increasing temperature, as the density of CO_2 decreased while the movement ability of polymer chains increased with increasing temperature, the sorption of CO_2 into PET also decreased. Therefore, this kinetics model is more suitable for the intrinsic hydrolysis reaction stage.

The effect of temperature

Figure 6 reveals the effect of temperature on the PET hydrolysis in $SCCO_2$. At each pressure for the time of 12 h, the D_h increased sharply with increasing temperature at the temperature range above 100°C, even the pressure was increased to 15 MPa, the D_h just reached to 53.00% at 100°C, while D_h already reached to 89.12% at 160°C and 8 MPa. Temperature can significantly affect the PET hydrolysis by changing the macroscopic property and chain structure of PET. When a polymer is in its glassy state, the movement of the polymer chains in the free volume is blocked, resulting in the size and distribution of the free volume of polymer are fixed.[69] Once the polymer changes from glassy to rubbery, the free volume of polymer and the energy of molecular thermodynamic movement are large enough for the polymer chains to move, and this effect conspicuously increases with increasing temperature till the polymer changes from solid to melted state. Hydrolysis in the solid polyesters is a complex process which highly depends on chain mobility of polyester and permeability of H_2O, whereas the scission of ester groups in the melted polyesters is an extremely rapid reaction.[45] It is advantageous for H_2O to contact with ester groups of melted PET, which can effectively enhance the PET hydrolysis. According to the reaction kinetics model of hydrolysis, a series of D_h data at high temperature, that is, above the melting point of PET, can be predicted, and the results are shown in Figure S7 of the Supporting Information. It can be found that elevated temperatures can effectively shorten the time required for the hydrolysis reaction, the dependence on CO_2 pressure of PET hydrolysis become weak at the temperature range above 200°C, especially, PET can be completely hydrolyzed within 5 h at any pressure.

The effect of CO_2 pressure

Figure 7 reveals the effect of pressure on the PET hydrolysis in $SCCO_2$. As discussed earlier, the effect of CO_2 pressure becomes weak at elevated temperatures, it can be found that the D_h increased slightly with increasing pressure at 160°C for 12 h, while D_h can be enhanced evidently at the temperature range of 100–130°C. As a compensating agent for the PET hydrolysis at low temperature, CO_2 plays a significant role in the solid PET due to the interaction between CO_2 and PET. As an electron acceptor, CO_2 can easily form

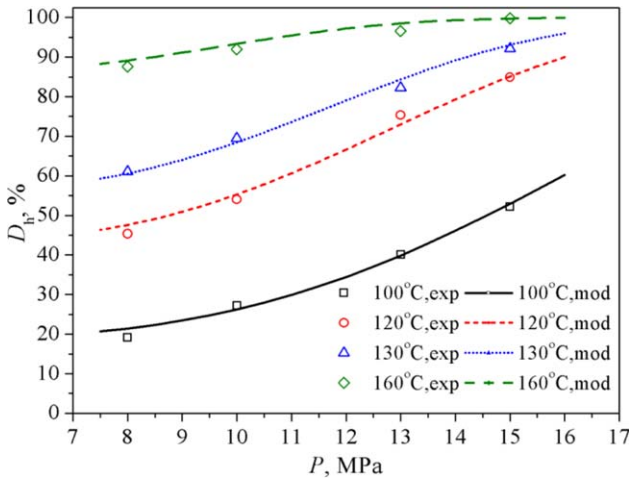

Figure 7. Degree of PET hydrolysis after 12 h vs. pressure at different temperatures.

[Color figure can be viewed in the online issue, which is available at wileyonlinelibrary.com.]

Table 3. Effect of Flake Size and Catalyst on the Degree of PET Hydrolysis at 160°C and 15 MPa

No.	System	Flake Size (mm^3)	t, h	D_h (%)
1	PET-catalyst-$SCCO_2$-H_2O	1 × 1 × 0.4	3	75.05
2	PET-catalyst-$SCCO_2$-H_2O	4 × 4 × 0.4	3	73.83
3	PET-catalyst-$SCCO_2$-H_2O	10 × 10 × 0.4	3	72.56
4	PET-catalyst-$SCCO_2$-H_2O	4 × 4 × 0.4	12	99.86
5	PET-catalyst-H_2O	4 × 4 × 0.4	12	41.33
6	PET-$SCCO_2$-H_2O	4 × 4 × 0.4	12	23.05

a complex with the oxygen in the carbonyl group of PET,[70] while this interaction decreases with increasing temperature, increases as the pressure increases, as the density of CO_2 increases steeply as the pressure increases. More H_2O carried by $SCCO_2$ can contact with ester groups by introducing concentrated $SCCO_2$ into the amorphous regions of PET matrix at low temperature, then improving the PET hydrolysis. Therefore, using CO_2 aims at optimizing operational conditions of the process and the process itself, and the effect of swelling can improve the kinetics as well as the mass-transport mechanism, as it increases the active surface of the solid polymer.[71]

The effect of the flake size and catalyst

A amount of references concluded that the apparent reaction rate of hydrolysis was proportional to the concentration of acid and inversely proportional to the initial diameter of the PET particles.[2,4,8,10] The degree of PET hydrolysis vs. different flake size at 160°C and 15 MPa for 3 h are shown in Table 3. Due to the PET used in this work was a flake, which thickness was only 0.4 mm, the size was determined by the surface area of flake, $SCCO_2$ could bring H_2O into the bulk of PET flake, therefore, the flake size had almost no effect on the hydrolysis. Conversely, the solid acid catalyst, SO_4^{2-}/TiO_2, used in this work could provide H_3O^+ by contacting with H_2O, with the transportation effect of $SCCO_2$, the H_3O^+ would induce the scission of ester groups, then accelerated the rate of hydrolysis. When catalyst or $SCCO_2$ absented from the reaction system, the hydrolysis would also be deteriorated, and the results were presented in Table 3. Therefore, both solid acid catalyst and $SCCO_2$ can improve the hydrolysis efficiency, the mechanism of PET hydrolysis using solid acid catalyst in $SCCO_2$ will be introduced in the next section.

Standard deviation analysis for the hydrolysis reaction kinetics model

To confirm the suitability, conformance, and effectiveness of this hydrolysis reaction kinetics model, the residual analysis and root-mean-square deviation analysis for the experimental values and model values were carried out. The results are shown in Table S4 of Supporting Information.

The differences between the experimental and model values ranges from 0.11% to 4.95%, and the standard deviation (σ_{D_h}) for D_h values was calculated by

$$\sigma_{D_h}=\sqrt{\frac{\sum_{1}^{N}{\delta_{D_h}}^2}{N-1}}=\sqrt{\frac{2.74\times10^{-2}}{56-1}}=2.23\times10^{-2} \quad (17)$$

Therefore, this reaction kinetics model provides an excellent description of the intrinsic hydrolysis of PET in $SCCO_2$.

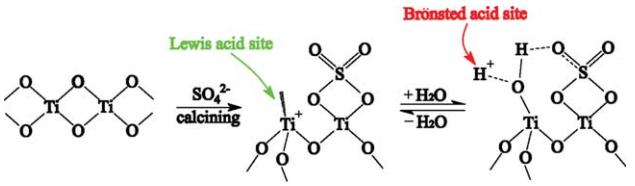

Figure 8. Schematic diagram of a sulfated titanium dioxide and the conversion of Lewis to Brönsted acid sites after H_2O adsorbed on the catalyst.

[Color figure can be viewed in the online issue, which is available at wileyonlinelibrary.com.]

Mechanism of the PET hydrolysis using SO_4^{2-}/TiO_2 catalyst in $SCCO_2$

Mechanism of the PET Hydrolysis Using SO_4^{2-}/TiO_2 Catalyst. After calcining the sulfated TiO_2, SO_4^{2-} anions linked to the framework of TiO_2 with the chelating bidentate form,[13,72,73] the schematic diagram could be found in Figure 8. Although the total acidity of catalyst would decrease appropriately (details are provided in the Supporting Information), the sulfated metal oxides showed larger surface area than that of the pure metal oxides, which provided more Lewis acid sites in the framework of TiO_2 so as to accommodate electrons from other molecules, this is the generation of the highly acidic property of SO_4^{2-}/TiO_2 catalyst.[13] Due to the hygroscopicity of SO_4^{2-}/TiO_2 catalyst, H_2O can adsorb on the framework of TiO_2, that is, the electron pairs of H_2O fill into the empty orbital of titanium cation, while the hydrogen cation will depart from H_2O to provide hydrogen proton to the chemical reaction, that is, the Brönsted acid site. This conversion of Lewis to Brönsted acid sites has been observed by FT-IR.[73] The presence of those Brönsted acid sites will make the acidic catalytic reactions occurred at lower temperature with the same rate as that occurred at higher temperature without catalyst.

The mechanism of acidic catalytic hydrolysis reaction of PET can be described in Figure 9. Hydrogen proton generated from acid catalyst randomly attacks the carbon atom of ester carbonyl group and makes it protonated rapidly, then carbonyl oxygen atom is converted into a secondary hydroxyl group. Subsequently, hydroxyl oxygen atom of water molecule slowly attacks the protonated carbon atom and combines with it, while hydrogen proton of water molecule combines with the oxygen atom of the ester bond to make it protonated due to the effect of hydrogen bond.

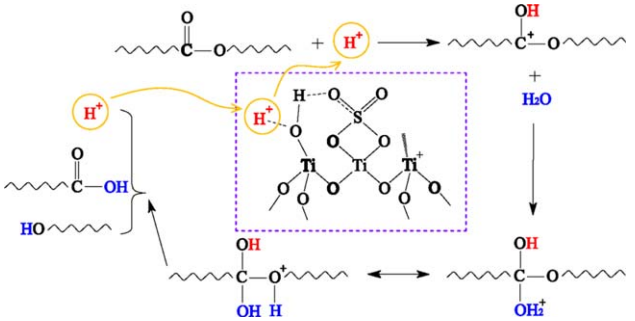

Figure 9. Mechanism of the PET hydrolysis using SO_4^{2-}/TiO_2 catalyst.

[Color figure can be viewed in the online issue, which is available at wileyonlinelibrary.com.]

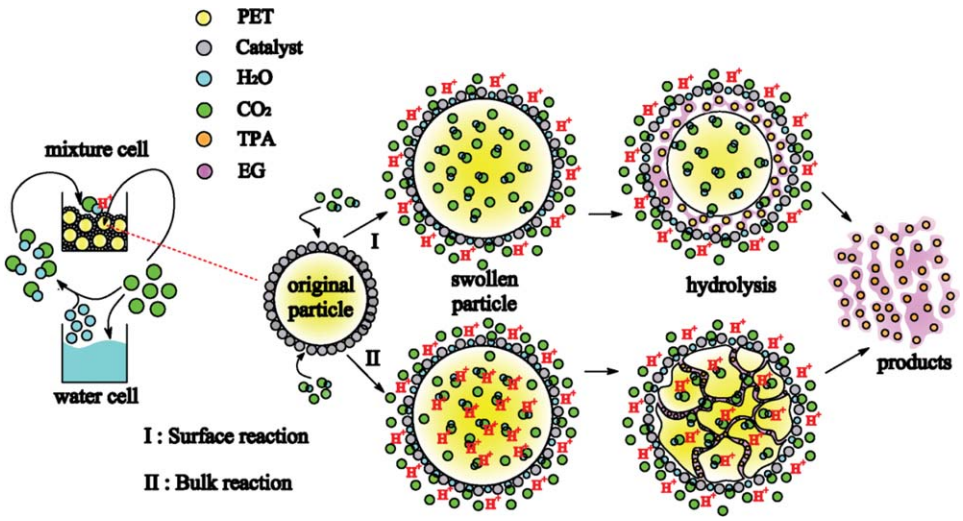

Figure 10. Schematic diagram of the mechanism of catalyzed PET hydrolysis with solid acid catalyst in $SCCO_2$.

H^+, which actually exists in the form of H_3O^+, represents the hydrogen proton generated from the SO_4^{2-}/TiO_2 catalyst by contacting with H_2O. [Color figure can be viewed in the online issue, which is available at wileyonlinelibrary.com.]

Finally, the ester bond is rapidly cleaved to generate the terminal carboxyl group and hydroxyl group, while hydrogen proton departs from the carbonyl oxygen and backs to the environment for the next reaction.[74,75] As hydrogen proton actually exists in the form of hydroniums, it can be suggested that two or more water molecules attack the ester bonds and induce the scission of chains of polyester, which accelerate the rate of hydrolysis.

Mechanism of the PET Hydrolysis in $SCCO_2$. A modified shrinking-core model has so far been known widely to describe the mechanism for the PET hydrolysis in H_2SO_4,[8] which suggested that the acid hydrolysis was a surface reaction, and the degree of hydrolysis was proportional to the surface area of the PET flakes. Furthermore, concentrated H_2SO_4 could lead to the formation of pores and cracks on the surface of PET flakes, which increased the effective surface area to accelerate the hydrolysis rate. Viana et al.[68] suggested that although the depolymerization was dependent on the reaction sites of PET surface, cleavage mainly occurred in the middle of chains during the initial period of reaction, monomer generated until the cleavage situated at the end of chains. However, in the $SCCO_2$-PET system, due to the swelling and carrying capacity of $SCCO_2$, the hydrolysis may occur on the surface or in the bulk of PET flakes, therefore, we assume two different paths to describe the mechanism of the acid hydrolysis of PET in $SCCO_2$, and the schematic diagram for this assumption is shown in Figure 10. Before CO_2 is supplied to the high-pressure vessel, the catalyst powder adheres on the surface of PET flakes, after heating and pressurizing the vessel to the experimental temperature and pressure, a small amount of $SCCO_2$ dissolves in H_2O and PET matrix to swell PET, conversely, some H_2O molecules are carried and transferred by $SCCO_2$ to the surface of PET/catalyst mixture and adsorbs on it to generate the hydroniums. Then, path I indicates that although parts of the H_2O molecules are carried by $SCCO_2$ and penetrate into the amorphous regions of the swollen PET, the hydroniums only stay on the surface of PET, then the hydrolysis occurs from surface to the core. Path II indicates that parts of the H_2O molecules as well as hydroniums are carried by $SCCO_2$ and penetrate into the amorphous regions of the swollen PET, then the hydrolysis occurs in the bulk of PET. Finally, the EG and TPA monomer will be obtained by this two different paths.

The most effective method of examining and confirming our assumption is to observe the morphology changes of the PET flake throughout the whole hydrolysis process. Here, we take the hydrolysis occurred at 160°C and 15 MPa for different time as a typical example to observe the actual situation of PET flake. Figures 11 and 12 show the morphology of the surface and the cross section of PET flake for the hydrolysis degree of 0, 39.21%, 73.83%, and 96.89%, as characterized by SEM, respectively. It could be seen from the inset images, due to the effects of the swelling of PET, deposition of the TPA product, and the CO_2-induced PET crystallization, the overall morphology and transparency of the PET flake surface had significantly changed accompanied by the hydrolysis. Clearly, formation of core and crack on the flake surface were observed at $D_h = 39.21\%$, then the crack gradually disappeared and became to a rough layer, while the cell-like morphology formed under the rough layer at $D_h = 73.83\%$, finally, when $D_h = 96.89\%$, almost all PET had been hydrolyzed, TPA product deposited and formed the cell-like surface morphology. For a similar phenomenon, the morphology of the cross section of flake also significantly changed accompanied by the hydrolysis. It is worth noting that the cell-like morphology could be observed clearly at the cross section of flake at $D_h = 73.83\%$, while the deposition of the TPA product expressed a slightly rough but not the cell-like morphology at $D_h = 96.89\%$. In fact, at the end of the hydrolysis reaction, TPA has been crystallized and exhibit the form of columnar polyhedron,[76] which can be observed in images S4-3a, S4-3b, and C4-3. Therefore, the acid hydrolysis of PET in $SCCO_2$ is not a single surface or bulk reaction but both of them.

To further investigate the process of acid hydrolysis of PET in $SCCO_2$, the plasticization and induced crystallization effects of CO_2 should be considered. Due to the CO_2 plasticization, the T_g and crystallization temperature of PET are depressed, which makes the mobility of polymer segments enhanced, and compared to the glassy state, the rubbery PET is more conducive to hydrolysis. Conversely, as the crystalline cross-links can stiffen and toughen the polymers, the

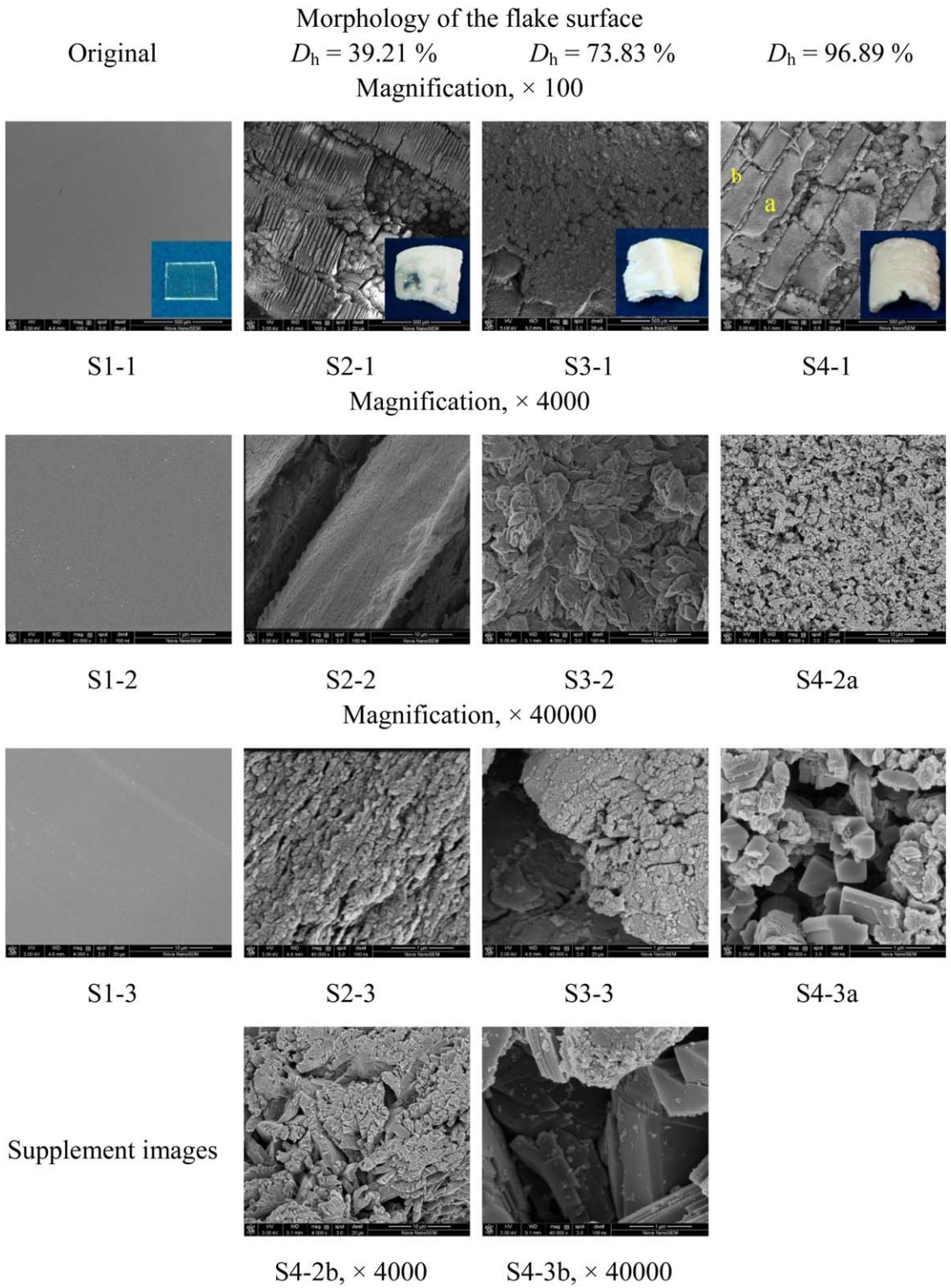

Figure 11. SEM characterization of the surface morphology change of PET flakes surface with magnification and degree of hydrolysis.

The color inset images in S1-1–S4-1 show the overall morphology of flakes. [Color figure can be viewed in the online issue, which is available at wileyonlinelibrary.com.]

crystalline region is more stable than the amorphous regions of polymer. The soft and random chain structure can degenerate easily, while the regular chain structure resist the degradation, therefore, the hydrolysis occurs in the amorphous regions of polymer prior to that in the crystalline region.[48] The chains of unreacted PET regularly rearrange to form crystalline region due to the effect of CO_2-induced crystallization. Interestingly, the distribution of amorphous regions and crystalline regions seems to exhibit a cell-like morphology, where the cell wall-like section is crystalline regions, and the cytoplasm-like section is the amorphous regions, therefore, image C3-2a exhibits more obviously evidence of

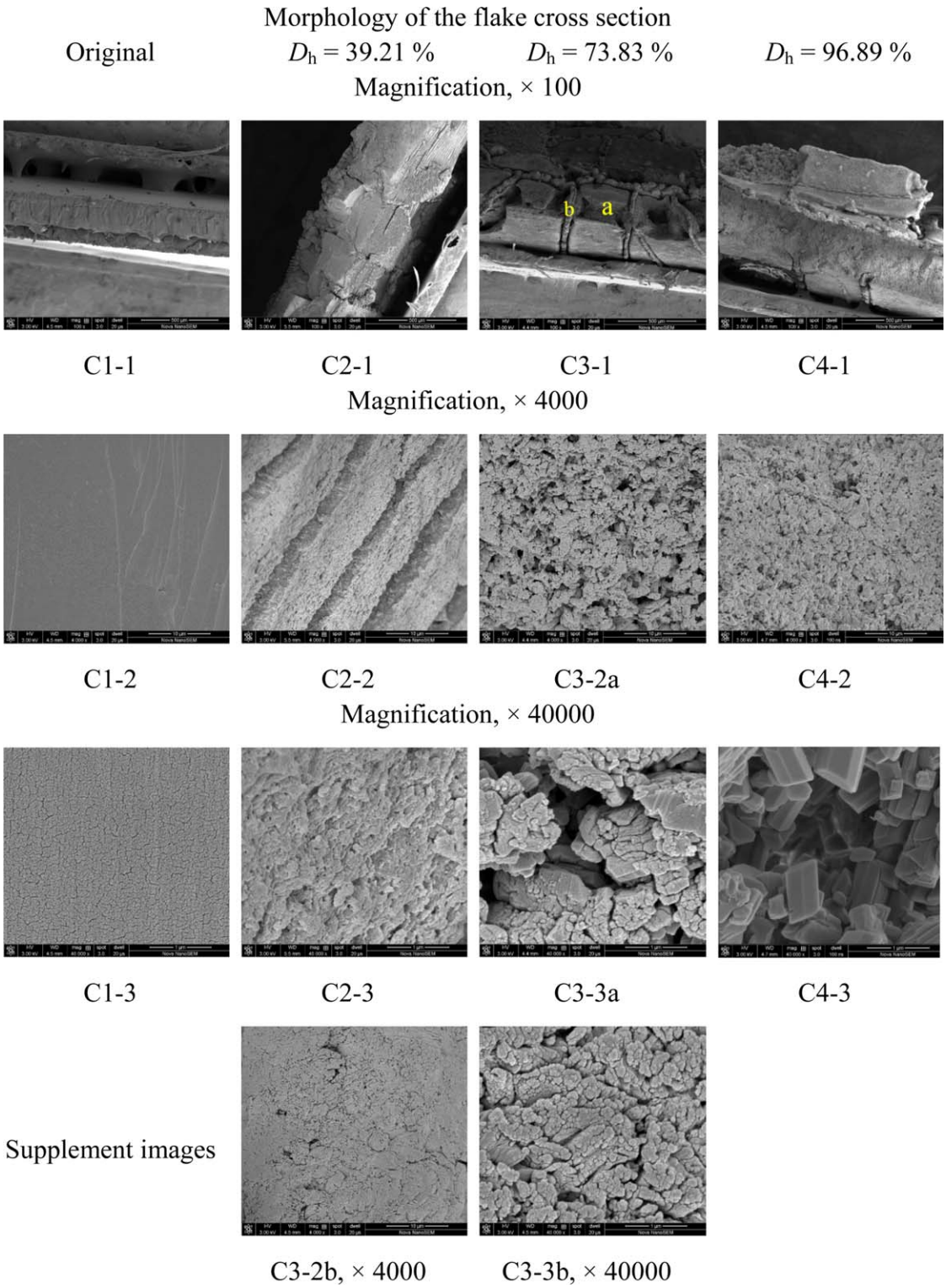

Figure 12. SEM characterization of the cross section morphology change of PET flakes surface with magnification and degree of hydrolysis.

[Color figure can be viewed in the online issue, which is available at wileyonlinelibrary.com.]

hydrolysis than that of image C3-2b, the similar phenomenon can be found between image S4-2a and S4-2b. Furthermore, the induced crystallization takes place from the flake surface to inside,[38] which makes the hydrolysis occur in the bulk of flake prior to that on the surface, therefore, when PET flake was almost completely hydrolyzed, after TPA depositing, the cell-like morphology can not be observed in the bulk of flake (image C4-1), where is only the TPA product (image C4-3), while the cell-like morphology can still be observed clearly at the flake surface (image S4-1), besides the number of crystals of TPA product in the cytoplasm-like section (S4-3a) is more than that in the cell wall-like section (S4-3b), and a little amount of unreacted PET also remains in this section.

In summary, the process of acid hydrolysis of PET in $SCCO_2$ can be described as follows, at the beginning, both water molecules and hydroniums are carried and then penetrate into the amorphous regions of PET matrix with the capability of swelling and diffusion of $SCCO_2$, simultaneously, mild hydrolysis reaction occurs on the surface and in the bulk of PET flakes, which results in the crack and pore appearing, and the rate of mild reaction on the surface is higher than that in the bulk. Subsequently with the plasticization and induced crystallization effect of $SCCO_2$, severe hydrolysis reaction preferentially carries out in the amorphous regions of PET, and the rate of severe reaction in the bulk becomes higher till the flakes will be hydrolyzed completely.

In the study of the degradation of polyesters, aliphatic polyesters are easier to be degraded,[7] while aromatic polyesters usually are regarded as biologically inert, such as PET.[77] The more flexible the main chain has, the higher the degradation rate is, otherwise, additives can also affect the degradation of polyesters.[75] Polyesters with low melting point are more susceptible to degradation than that with high melting point, such as it is difficult to degrade the nylon 66 due to the effect of the intermolecular hydrogen bonds in amide groups.[78] For the conventional concept of the polyester hydrolysis in strong liquid acid, the hydrolytic attack occurred preferentially at chain ends through external diffusion-kinetic conditions (mainly on the surface), which was controlled by the mechanism of strong acid diffusion into the polymer structure.[56] However, with the assistance of $SCCO_2$, the mechanism for the degradation of polyesters will be a combination of bulk and surface reaction, which is controlled by the capacity of the swelling, diffusion, and induced crystallization of CO_2.

One of the effective ways to improve the efficiency of polyester degradation is to enhance the mobility of polyester chain segments. As the most widely used SCF, $SCCO_2$ plays an important role in this way, besides microwave irradiation or ultrasonic treatment also can enhance the mobility of polyester chain segments.[53,79–82] Another effective way is to increase the effective surface area of polyester specimens, that is, to pretreat the surface or inside of the specimens before degradation, such as reducing the diameter of PET particles and using $SCCO_2$ to swell the PET specimens, while the plasma surface treatment can increase both surface area and hydrophilicity of PET specimens.[83]

It is reasonable to assume that other chemical degradation methods took place in $SCCO_2$ will improve the efficiency due to the excellent modification and carrying capacity of $SCCO_2$. For instance, in the methanolysis process, there is no need to reach the desired reaction temperature and pressure of supercritical methanol, $SCCO_2$ can carry methanol and then diffuse into the inside of polyester to make the bulk reaction occurred, of course, further experimental attempts in the future will be needed to verify these assumption.

Conclusions

The waste PET bottles could be almost completely hydrolyzed to monomers of TPA, EG and a little amount of DEG at 160°C and 15 MPa after 12 h with SO_4^{2-}/TiO_2 catalyst in $SCCO_2$, the scission of ester groups in PET long chains occurred at both chain end and random chain due to the assistance of $SCCO_2$. The reaction kinetics model of PET hydrolysis in $SCCO_2$ was detected using the experimental data over the ranges of 8–15 MPa, 100–160°C, and 3–12 h, and the model agreed very well with all the experimental data, as the standard deviation was 2.23×10^{-2}, except for that in the time range of 0–3 h, where the effect of swelling of PET were more significant than the hydrolysis reaction of PET. The frequency factor was proportional to temperature and apparent activation energy (E) was inversely proportional to the pressure. In whole process of hydrolysis, temperature could significantly affect the PET hydrolysis by changing the macroscopic property and chain structure of PET, pressure improved hydrolysis efficiency by increasing the density of $SCCO_2$ to transfer more H_2O and H_3O^+, generated from solid acid catalyst by contacting with H_2O, to the PET matrix, while the PET flake size had almost no effect on the hydrolysis efficiency.

The mechanism of the PET hydrolysis in $SCCO_2$ was a combination of bulk and surface reaction, which could be described by two steps. At the beginning, both water molecules and hydroniums were carried and then penetrated into the amorphous regions of the swelling PET by $SCCO_2$, the rate of mild hydrolysis reaction was higher at the PET flake surface. Subsequently severe hydrolysis reaction preferentially took place in the amorphous regions of PET, with the plasticization and induced crystallization effect of $SCCO_2$, the rate of bulk reaction became higher till the flakes would be hydrolyzed completely.

Acknowledgment

This work is supported by the National Natural Science Foundation of China (NSFC), Grant numbers: 20676031 and 20876051.

Literature Cited

1. Dimitrov N, Kratofil KL, Ptiček SA, Hrnjak-Murgić Z. Analysis of recycled PET bottles products by pyrolysis-gas chromatography. *Polym Degrad Stab*. 2013;98:972–979.
2. Sinha V, Patel M, Patel J. Pet waste management by chemical recycling: a review. *J Polym Environ*. 2010;18:8–25.
3. Achilias DS, Karayannidis GP. The chemical recycling of PET in the framework of sustainable development. *Water Air Soil Pollut Focus*. 2004;4:385–396.
4. Karayannidis GP, Achilias DS. Chemical recycling of poly(ethylene terephthalate). *Macromol Mater Eng*. 2007;292:128–146.
5. Paszun D, Spychaj T. Chemical recycling of poly(ethylene terephthalate). *Ind Eng Chem Res*. 1997;36:1373–1383.
6. Campanelli JR, Kamal MR, Cooper DG. A kinetic study of the hydrolytic degradation of polyethylene terephthalate at high temperatures. *J Appl Polym Sci*. 1993;48:443–451.
7. Lin C-C, Guo G-L, Tsai T-L. A bi-order kinetic model for poly (methyl methacrylate) decomposition in HNO_3 using microwave irradiation. *AIChE J*. 2009;55:2150–2158.
8. Yoshioka T, Motoki T, Okuwaki A. Kinetics of hydrolysis of poly (ethylene terephthalate) powder in sulfuric acid by a modified shrinking-core model. *Ind Eng Chem Res*. 2001;40:75–79.
9. Yoshioka T, Okayama N, Okuwaki A. Kinetics of hydrolysis of PET powder in nitric acid by a modified shrinking-core model. *Ind Eng Chem Res*. 1998;37:336–340.
10. Mishra S, Goje AS, Zope VS. Chemical recycling, kinetics, and thermodynamics of hydrolysis of poly(ethylene terephthalate) (PET) waste in sulfuric acid in presence of phosphoric acid. *Polym Plast Technol Eng*. 2003;42:581–603.
11. Liu F, Cui X, Yu S, Li Z, Ge X. Hydrolysis reaction of poly(ethylene terephthalate) using ionic liquids as solvent and catalyst. *J Appl Polym Sci*. 2009;114:3561–3565.
12. Zhang L, Gao J, Zou J, Yi F. Hydrolysis of poly(ethylene terephthalate) waste bottles in the presence of dual functional phase transfer catalysts. *J Appl Polym Sci*. 2013;130:2790–2795.

13. Corma A. Inorganic solid acids and their use in acid-catalyzed hydrocarbon reactions. *Chem Rev*. 1995;95:559–614.
14. Corma A. Solid acid catalysts. *Curr Opin Solid State Mater Sci*. 1997;2:63–75.
15. Aydemir B, Aslı Sezgi N, Doğu T. Synthesis of TPA impregnated SBA-15 catalysts and their performance in polyethylene degradation reaction. *AIChE J*. 2012;58:2466–2472.
16. Song X, Zhang S, Zhang D. Catalysis investigation of PET depolymerization under metal oxides by microwave irradiation. *J Appl Polym Sci*. 2010;117:3155–3159.
17. Wang PC, Zhu J, Liu X, Lu TT, Lu M. Regioselective nitration of aromatics with nanomagnetic solid superacid SO_4^{2-}/ZrO_2-M_xO_y-Fe_3O_4 and its theoretical studies. *ChemPlusChem*. 2013;78:310–317.
18. Sharma YC, Singh B, Korstad J. Advancements in solid acid catalysts for ecofriendly and economically viable synthesis of biodiesel. *Biofuels Bioprod Biorefin*. 2011;5:69–92.
19. Shen X, Wang YX, Hu CW, Qian K, Ji Z, Jin M. One-pot conversion of inulin to furan derivatives catalyzed by sulfated TiO_2/mordenite solid acid. *ChemCatChem*. 2012;4:2013–2019.
20. Matsuhashi H, Miyazaki H, Kawamura Y, Nakamura H, Arata K. Preparation of a solid superacid of sulfated tin oxide with acidity higher than that of sulfated zirconia and its applications to aldol condensation and benzoylation1. *Chem Mater*. 2001;13:3038–3042.
21. Corma A, Fornés V, Juan-Rajadell MI, Nieto JML. Influence of preparation conditions on the structure and catalytic properties of SO_4^{2-}/ZrO_2 superacid catalysts. *Appl Catal A*. 1994;116:151–163.
22. Adschiri T, Sato O, Machida K, Saito N, Arai K. Recovery of terephthalic acid by decomposition of PET in supercritical water. *Kag Kog Ronbunshu*. 1997;23:505–511.
23. Arai K. Conversion of polymers and biomass to chemical intermediates with supercritical water. *Macromol Symposia*. 1998;135:205–214.
24. Goto M. Chemical recycling of plastics using sub- and supercritical fluids. *J Supercrit Fluids*. 2009;47:500–507.
25. Goto M, Koyamoto H, Kodama A, Hirose T, Nagaoka S, McCoy BJ. Degradation kinetics of polyethylene terephthalate in supercritical methanol. *AIChE J*. 2002;48:136–144.
26. Genta M, Yano F, Kondo Y, Matsubara W, Oomoto S. Development of chemical recycling process for post-consumer PET bottle by methanolysis in supercritical methanol. *Tech Rev*. 2003;40:1–4.
27. Genta M, Iwaya T, Sasaki M, Goto M, Hirose T. Depolymerization mechanism of poly(ethylene terephthalate) in supercritical methanol. *Ind Eng Chem Res*. 2005;44:3894–3900.
28. Goto M, Sasaki M, Hirose T. Reactions of polymers in supercritical fluids for chemical recycling of waste plastics. *J Mater Sci*. 2006;41:1509–1515.
29. Chiou JS, Barlow JW, Paul DR. Polymer crystallization induced by sorption of CO_2 gas. *J Appl Polym Sci*. 1985;30:3911–3924.
30. Goel SK, Beckman EJ. Nucleation and growth in microcellular materials: supercritical CO_2 as foaming agent. *AIChE J*. 1995;41:357–367.
31. Li D-C, Liu T, Zhao L, Lian X-S, Yuan W-K. Foaming of poly(lactic acid) based on its nonisothermal crystallization behavior under compressed carbon dioxide. *Ind Eng Chem Res*. 2011;50:1997–2007.
32. Li D-C, Liu T, Zhao L, Yuan W-K. Solubility and diffusivity of carbon dioxide in solid-state isotactic polypropylene by the pressure−decay method. *Ind Eng Chem Res*. 2009;48:7117–7124.
33. Bonavoglia B, Storti G, Morbidelli M, Rajendran A, Mazzotti M. Sorption and swelling of semicrystalline polymers in supercritical CO_2. *J Polym Sci B*. 2006;44:1531–1546.
34. Wissinger RG, Paulaitis ME. Swelling and sorption in polymer–CO_2 mixtures at elevated pressures. *J Polym Sci B*. 1987;25:2497–2510.
35. Tomasko DL, Li H, Liu D, Han X, Wingert MJ, Lee LJ, Koelling KW. A review of CO_2 applications in the processing of polymers. *Ind Eng Chem Res*. 2003;42:6431–6456.
36. Chiou JS, Barlow JW, Paul DR. Plasticization of glassy polymers by CO_2. *J Appl Polym Sci*. 1985;30:2633–2642.
37. Koros WJ, Paul DR. CO_2 sorption in poly(ethylene terephthalate) above and below the glass transition. *J Polym Sci Polym Phys Ed*. 1978;16:1947–1963.
38. Li D, Liu T, Zhao L, Yuan W. Controlling sandwich-structure of PET microcellular foams using coupling of CO_2 diffusion and induced crystallization. *AIChE J*. 2012;58:2512–2523.
39. Takada M, Ohshima M. Effect of CO_2 on crystallization kinetics of poly(ethylene terephthalate). *Polym Eng Sci*. 2003;43:479–489.
40. von Schnitzler J, Eggers R. Mass transfer in polymers in a supercritical CO_2-atmosphere. *J Supercrit Fluids*. 1999;16:81–92.
41. Sorrentino L, Di Maio E, Iannace S. Poly(ethylene terephthalate) foams: correlation between the polymer properties and the foaming process. *J Appl Polym Sci*. 2010;116:27–35.
42. Zhang Z, Handa YP. An in situ study of plasticization of polymers by high-pressure gases. *J Polym Sci B*. 1998;36:977–982.
43. Lambert SM, Paulaitis ME. Crystallization of poly(ethylene terephthalate) induced by carbon dioxide sorption at elevated pressures. *J Supercrit Fluids*. 1991;4:15–23.
44. Bratek W, Świątkowski A, Pakuła M, Biniak S, Bystrzejewski M, Szmigielski R. Characteristics of activated carbon prepared from waste PET by carbon dioxide activation. *J Anal Appl Pyrolysis*. 2013;100:192–198.
45. Carta D, Cao G, D'Angeli C. Chemical recycling of poly(ethylene terephthalate) (pet) by hydrolysis and glycolysis. *Environ Sci Pollut Res*. 2003;10:390–394.
46. Uhlmann DR. A kinetic treatment of glass formation. *J Non-Cryst Solids*. 1972;7:337–348.
47. SuriÑach S, Baro MD, Clavaguera-Mora MT, Clavaguera N. Glass formation and crystallization in the GeSe2-Sb2Te3 system. *J Mater Sci*. 1984;19:3005–3012.
48. Zhang R-H, Li X-K, Cao G-P, Shi Y-H, Liu H-L, Yuan W-K, Roberts GW. Improved kinetic model of crystallization for isotactic polypropylene induced by supercritical CO_2: introducing pressure and temperature dependence into the Avrami equation. *Ind Eng Chem Res*. 2011;50:10509–10515.
49. Ciric AR, Miao P. Steady state multiplicities in an ethylene glycol reactive distillation column. *Ind Eng Chem Res*. 1994;33:2738–2748.
50. Broeker J, Macek J, Rosen B, Bartos T. Process for recovery of aromatic acid from waste polyester resin. 1995. US Patent 5,414,113.
51. Tustin G, Pell T Jr, Jenkins D, Jernigan M. Process for the recovery of terephthalic acid and ethylene glycol from poly(ethylene terephthalate). 1995. US Patent 5,413,681.
52. Bartos T, Rosen B, Rosenfeld J. Process for recovery of aromatic acid or ester and polyol from waste polyester resins. 1996. US Patent 5,502,247.
53. Siddiqui MN, Achilias DS, Redhwi HH, Bikiaris DN, Katsogiannis KAG, Karayannidis GP. Hydrolytic depolymerization of PET in a microwave reactor. *Macromol Mater Eng*. 2010;295:575–584.
54. Li X-K, Lu H, Cao G-P, Qian Y-H, Chen L-H, Zhang R-H, Liu H-L, Shi Y-H. Experimental study of the synergistic plasticizing effect of carbon dioxide and ibuprofen on the glass transition temperature of poly(methyl methacrylate). *Ind Eng Chem Res*. 2014.
55. Imran M, Kim B-K, Han M, Cho BG, Kim DH. Sub- and supercritical glycolysis of polyethylene terephthalate (PET) into the monomer bis(2-hydroxyethyl) terephthalate (BHET). *Polym Degrad Stab*. 2010;95:1686–1693.
56. Mancini SD, Zanin M. Post consumer pet depolymerization by acid hydrolysis. *Polym Plast Technol Eng*. 2007;46:135–144.
57. Ballara A, Verdu J. Physical aspects of the hydrolysis of polyethylene terephthalate. *Polym Degrad Stab*. 1989;26:361–374.
58. Launay A, Thominette F, Verdu J. Hydrolysis of poly(ethylene terephthalate): a kinetic study. *Polym Degrad Stab*. 1994;46:319–324.
59. Middleton AC, Duckett RA, Ward IM, Mahendrasingam A, Martin C. Real-time FTIR and WAXS studies of drawing behavior of poly (ethylene terephthalate) films. *J Appl Polym Sci*. 2001;79:1825–1837.
60. Lu XF, Hay JN. Crystallization orientation and relaxation in uniaxially drawn poly(ethylene terephthalate). *Polymer*. 2001;42:8055–8067.
61. Holland BJ, Hay JN. The thermal degradation of PET and analogous polyesters measured by thermal analysis–Fourier transform infrared spectroscopy. *Polymer*. 2002;43:1835–1847.
62. McCoy BJ, Madras G. Degradation kinetics of polymers in solution: dynamics of molecular weight distributions. *AIChE J*. 1997;43:802–810.
63. Causin V, Marega C, Guzzini G, Marigo A. Forensic analysis of poly(ethylene terephthalate) fibers by infrared spectroscopy. *Appl Spectrosc*. 2004;58:1272–1276.
64. Téllez CA, Hollauer E, Mondragon MA, Castaño VM. Fourier transform infrared and Raman spectra, vibrational assignment and ab initio calculations of terephthalic acid and related compounds. *Spectrochim Acta A*. 2001;57:993–1007.
65. Pickett JE, Coyle DJ. Hydrolysis kinetics of condensation polymers under humidity aging conditions. *Polym Degrad Stab*. 2013;98:1311–1320.
66. Mishra S, Zope VS, Goje AS. Kinetics and thermodynamics of hydrolytic depolymerization of poly(ethylene terephthalate) at high pressure and temperature. *J Appl Polym Sci*. 2003;90:3305–3309.

67. Karayannidis GP, Chatziavgoustis AP, Achilias DS. Poly(ethylene terephthalate) recycling and recovery of pure terephthalic acid by alkaline hydrolysis. *Adv Polym Tech*. 2002;21:250–259.
68. Viana ME, Riul A, Carvalho GM, Rubira AF, Muniz EC. Chemical recycling of PET by catalyzed glycolysis: kinetics of the heterogeneous reaction. *Chem Eng J*. 2011;173:210–219.
69. Li X-K, Cao G-P, Chen L-H, Zhang R-H, Liu H-L, Shi Y-H. Study of the anomalous sorption behavior of CO_2 into poly(methyl methacrylate) films in the vicinity of the critical pressure and temperature using a quartz crystal microbalance (QCM). *Langmuir*. 2013;29:14089–14100.
70. Kazarian SG, Vincent MF, Bright FV, Liotta CL, Eckert CA. Specific intermolecular interaction of carbon dioxide with polymers. *J Am Chem Soc*. 1996;118:1729–1736.
71. Piñero-Hernanz R, García-Serna J, Cocero MJ. Nonstationary model of the semicontinuous depolymerization of polycarbonate. *AIChE J*. 2006;52:4186–4199.
72. de Almeida RM, Noda LK, Gonçalves NS, Meneghetti SMP, Meneghetti MR. Transesterification reaction of vegetable oils, using superacid sulfated TiO_2–base catalysts. *Appl Catal A*. 2008;347:100–105.
73. Arata K, Hino M. Solid catalyst treated with anion: XVIII. Benzoylation of toluene with benzoyl chloride and benzoic anhydride catalysed by solid superacid of sulfate-supported alumina. *Appl Catal*. 1990;59:197–204.
74. Otton J, Ratton S, Vasnev VA, Markova GD, Nametov KM, Bakhmutov VI, Komarova LI, Vinogradova SV, Korshak VV. Investigation of the formation of poly(ethylene terephthalate) with model molecules: kinetics and mechanisms of the catalytic esterification and alcoholysis reactions. II. Catalysis by metallic derivatives (monofunctional reactants). *J Polym Sci A*. 1988;26:2199–2224.
75. Scheirs J, Long TE. *Modern Polyesters: Chemistry and Technology of Polyesters and Copolyesters*. New York: Wiley, 2004.
76. Davey RJ, Maginn SJ. Morphology and polymorphism in molecular crystals: terephthalic acid. *J Chem Soc Faraday Trans*. 1994;90:1003–1009.
77. Mueller R-J. Biological degradation of synthetic polyesters—enzymes as potential catalysts for polyester recycling. *Process Biochem*. 2006;41:2124–2128.
78. Steppan DD, Doherty MF, Malone MF. A simplified degradation model for nylon 6,6 polymerization. *J Appl Polym Sci*. 1991;42:1009–1021.
79. Sivalingam G, Agarwal N, Madras G. Kinetics of microwave-assisted oxidative degradation of polystyrene in solution. *AIChE J*. 2003;49:1821–1826.
80. Sivalingam G, Agarwal N, Madras G. Distributed midpoint chain scission in ultrasonic degradation of polymers. *AIChE J*. 2004;50:2258–2265.
81. Marimuthu A, Madras G. Continuous distribution kinetics for microwave-assisted oxidative degradation of poly(alkyl methacrylates). *AIChE J*. 2008;54:2164–2173.
82. Madras G, McCoy BJ. Molecular-weight distribution kinetics for ultrasonic reactions of polymers. *AIChE J*. 2001;47:2341–2348.
83. Mancini SD, Nogueira AR, Rangel EC, da Cruz NC. Solid-state hydrolysis of postconsumer polyethylene terephthalate after plasma treatment. *J Appl Polym Sci*. 2013;127:1989–1996.

Manuscript received Apr. 4, 2014, and revision received Aug. 17, 2014.